Kinetics of the Dissolution of Magnetite in Thioglycolic Acid Solutions †

By **Erwin Baumgartner, Miguel A. Blesa,* and Alberto J. G. Maroto,** Departamento Química de Reactores, Comisión Nacional de Energía Atómica, Buenos Aires, Argentina

The kinetics of the dissolution of magnetite by thioglycolic acid (mercaptoacetic acid) have been studied at different acid concentrations and specific surface areas, and as a function of pH and temperature. The experimental evidence points to the overall rate of reaction depending on the instantaneous surface area of the magnetite particles and that the probable reaction mechanism is the decomposition of the species formed by the interaction of thioglycolate anion with the protonated OH groups located on the surface of the magnetite particles. This mechanism explains the sharp maximum in the dissolution rate constant obtained at pH *ca.* 4.5, as it takes into account two phenomena which are sensitive to pH in opposite directions, the increase in thioglycolate anion concentration as the pH is increased and the increase in the amount of protonated superficial OH groups as the pH is lowered. The activation enthalpy for this reaction was found to be 15.5 kJ mol^{-1}.

MAGNETITE, Fe_3O_4, is usually found in the oxide layers grown on carbon steel under hydrothermal conditions,[1] in a relatively reducing environment.[2] It is also found on stainless steels,[3] although in this case nickel ferrite, $Ni_xFe_{3-x}O_4$ ($x \leqslant 1$) is often the most important phase.

Removal of the oxide layer from the base metal may become necessary, for instance, for the oxide layers containing radionuclides such as ^{60}Co formed [4-7] in nuclear reactors. It can be dissolved using two types of reactions of magnetite: [2,4,8,9] (*i*) by using strong reductants, such as H_2 or V^{II} complexes,[8] or (*ii*) acid dissolution assisted by complexation of the iron(II) and/or iron(III) ions released using mixtures of polycarboxylic acids, such as ethylenediaminetetra-acetic acid (H_4edta), nitrilotriacetic acid (H_3nta), oxalic, and citric acids. Under actual decontamination conditions, the reaction may be controlled by the mass-transfer stage, especially when diluted reagents are used,[10] but the chemical or physicochemical interactions are limiting in many instances. For example, in the interaction of H_4edta with iron(III) oxides,[11] adsorption and dissolution can be observed as different phenomena taking place at different pH's. For the magnetite–H_4edta interaction, it is more difficult to separate both phenomena.[12,13]

Thioglycolate (mercaptoacetate) is a very strong complexing ion for iron, especially in alkali media. It complexes both iron(II) and iron(III) ions [14-16] and reduces the latter by intramolecular electron transfer with formation of disulphide, $^-O_2CCH_2SSCH_2CO_2^-$, as it has been demonstrated in homogeneous media.[15,16] The reaction for the dissolution of magnetite by thioglycolic acid (mercaptoacetic acid) in deaerated solutions is represented by equation (I).[15] In the presence of dissolved

$$Fe_3O_4 + 5\ HSCH_2CO_2H \longrightarrow 3\ Fe(SCH_2CO_2) + HO_2CCH_2SSCH_2CO_2H + 4\ H_2O \quad (I)$$

oxygen a dynamic interconversion $Fe^{II} \rightleftharpoons Fe^{III}$ is established, which is the basis of the colorimetric determination of total iron by thioglycolic acid.[14,16]

In this paper we present a kinetic study of the dissolution of magnetite by thioglycolic acid. Apart from their practical importance, the results also suggest some general considerations which should be applicable to the dissolution of other oxides by acid solutions containing complexing ions.

† Presented in part at the 7th Scientific Meeting of the Argentine Nuclear Technology Association, Mendoza, 1978.

EXPERIMENTAL

The reagents employed were all of analytical purity or better, and were used as provided. Magnetite was prepared as described in a previous paper,[17] by reaction of potassium nitrate with a slurry of iron(II) hydroxide in the presence of hydrazine. It was characterized by its powder *X*-ray diffractogram, Mössbauer spectroscopy,[18,19] and scanning electron microscopy (s.e.m.). Except for the kinetic runs where the influence of specific surface area was investigated, a magnetite sample having an average particle diameter of 0.17 μm was used; its specific surface area, as obtained by nitrogen adsorption and Brunauer, Emmett, and Teller procedure, was 10 $m^2\ g^{-1}$. Special care was taken in determining stoicheiometry and purity through Mössbauer spectroscopy and s.e.m.[17,18,20]

Kinetic experiments were performed in a cylindrical beaker provided with a water jacket and stirred magnetically. Magnetite (20 mg) was suspended in doubly distilled water in an ultrasonic bath. Thermostatted solutions of thioglycolic acid and sodium hydroxide (enough to obtain the desired pH) were added. Periodical sampling was performed by means of a syringe; these samples were poured into a large volume of water containing thioglycolic acid and ammonia in excess. This solution was filtered through a Nuclepore membrane (pore size 0.45 μm) and the absorbance of the red complex at 530 nm was measured with a Shimadzu UV-210 A spectrophotometer. The amount of dissolved iron was then calculated from the calibration curve [$\varepsilon = (3.96 \pm 0.01) \times 10^2\ m^2\ mol^{-1}$].

RESULTS AND DISCUSSION

The results obtained are shown in Figures 1 and 2 in the form of dissolved iron fraction, f (amount of dissolved iron divided by total iron). Figure 1 shows a series of curves of f as a function of time at different pH values, at 30 °C. Figure 2 shows a series of curves of f as a function of time at different temperatures, at pH = 4.0.

The values plotted correspond to stirring rates above a

certain threshold value (around 250 r.p.m.); below this value, the rate of reaction increased as the stirring rate increased. We concentrated on the region where mass transfer is certainly not rate determining, *i.e.* at the higher stirring rate. It should be noted that below the

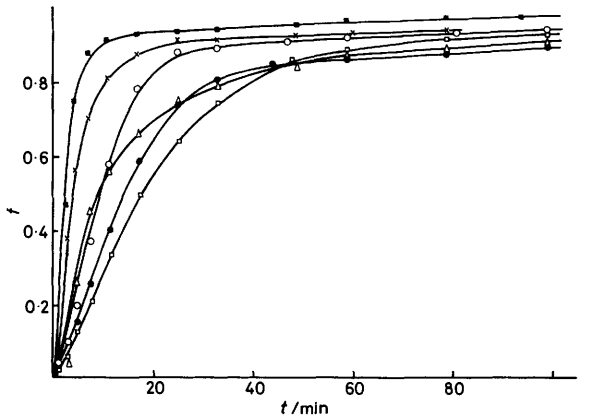

FIGURE 1 Dissolved iron fraction (f) as a function of time (t) at pH 2.08 (□), 2.69 (●), 3.46 (○), 4.60 (■), 5.22 (×), and 6.02 (△). [$HSCH_2CO_2H$] = 0.735 mol dm^{-3}; temperature (T) = 30 °C

threshold stirring rate, mass transfer is not necessarily rate determining, as surface reactions and mass transfer to bulk may be coupled phenomena.[21]

In Figure 3 the values of Figure 1 are plotted in the form $1 - (1 - f)^{\frac{1}{3}}$ *versus* time.[22] The plots obtained are linear, at least up to a dissolved iron fraction of 0.7. This indicates that the overall reaction is proportional to the instantaneous surface area S, as shown in equations (1)—(6), for a spherical particle of instantaneous mass m. Using the expression (2) equation (3) is obtained, which on integration gives equation (4). For nN_A identical

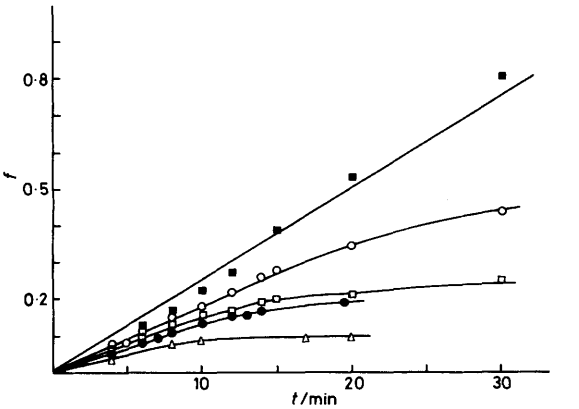

FIGURE 2 Dissolved iron fraction (f) as a function of time at different temperatures: T = 80 (■), 70 (○), 50 (□), 40 (●), and 30 °C (△). [$HSCH_2CO_2H$] = 0.524 mol dm^{-3}; pH 4.0

$$-\mathrm{d}m/\mathrm{d}t = k_s S = 4\pi k_s r^2 \quad (1)$$

$$m = (4\pi\rho r^3)/3 \quad (2)$$

$$-\mathrm{d}r/\mathrm{d}t = k_s\rho^{-1} \quad (3)$$

$$r_0 - r = k_s\rho^{-1}t \quad (4)$$

spherical particles, which will have a mass $M = nN_Am$, equation (5) may be obtained. Substituting $f = 1 - M/M_0$ gives equation (6), valid for a fixed initial magnetite mass, M_0. According to this derivation, the validity of the well known equation (6) rests upon the basic assumption of N identical spherical particles, in which geometrical and specific surface areas are equal. The magnetite employed in this study was polydisperse; this does not, however, affect the validity of equation

$$[(4\pi nN_A\rho)/3]^{\frac{1}{3}}(r_0 - r) = M_0^{\frac{1}{3}} - M^{\frac{1}{3}} = k't \quad (5)$$

$$1 - (1 - f)^{\frac{1}{3}} = k't/(M_0)^{\frac{1}{3}} = kt \quad (6)$$

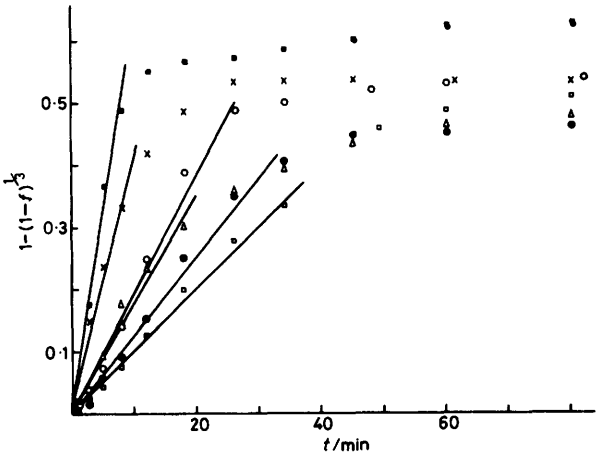

FIGURE 3 $1 - (1 - f)^{\frac{1}{3}}$ as a function of t at pH 2.08 (□), 2.69 (●), 3.46 (○), 4.60 (■), 5.22 (×), and 6.02 (△). [$HSCH_2CO_2H$] = 0.735 mol dm^{-3}; T = 30 °C

(6), as it has been shown [23] that in the case of the dissolution of hematite the width of the particle size distribution curve does not significantly change the amount reacted *versus* time profile.

Rate constants k were obtained, according to equation (6), by least-squares analysis of the linear portion of the plots of $1 - (1 - f)^{\frac{1}{3}}$ *versus* time.

Additional experiments were carried out on magnetite samples of different particle sizes. The rate constant for the dissolution of magnetite depends linearly on the specific surface area of the oxide, obtained by gas adsorption, as shown in Figure 4, thus confirming the assumption used in the derivation of equation (6). Actually, the geometrical model used for this derivation predicts a linear relationship between the rate constant and the geometrical surface area, instead of the specific surface area, but s.e.m. pictures demonstrated that the materials employed in this study were highly crystalline, and that geometrical and specific surface areas, although not equal, were close and proportional to each other.

The influence of the concentration of thioglycolic acid on the rate constant k is shown in Figure 5. As k is proportional to the dissolution rate per unit surface area [see equation (6)], its dependence on the concentration of thioglycolic acid (practically equal to its equilibrium concentration, since the amount adsorbed on magnetite

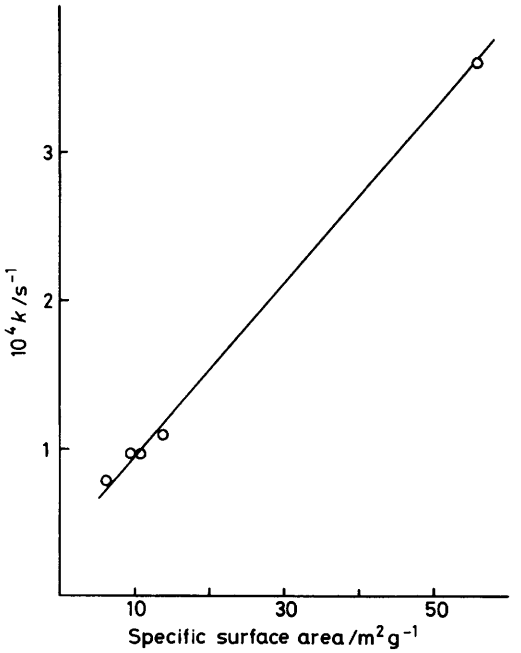

FIGURE 4 Dissolution rate constant k of magnetite as a function of the specific surface area of the oxide. $[HSCH_2CO_2H]$ = 0.147 mol dm^{-3}; T = 30 °C; pH 2.5

particles is negligible) can be interpreted as arising from a fast adsorption equilibrium, governed by a Langmuir type adsorption isotherm, preceding the rate-determining step; this is a well known fact in heterogeneous kinetics.[24]

The rate constant of the dissolution is highly dependent upon the pH of the solution. A sharp maximum in rate is achieved at pH *ca.* 4.5, as shown in Figure 6.

The sharp maximum is the result of a mechanism involving two phenomena which are sensitive to pH in opposite directions. The increase in the rate as the pH

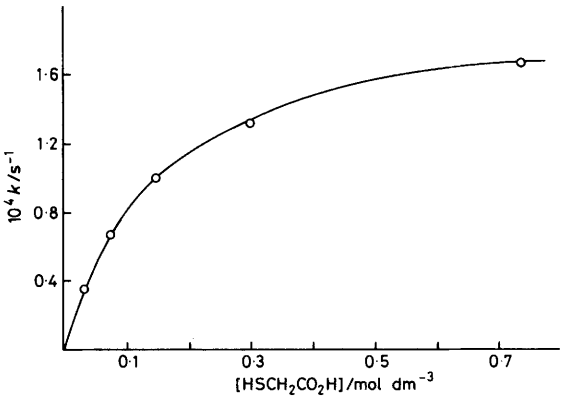

FIGURE 5 Influence of concentration of thioglycolic acid on the dissolution rate constant k of magnetite at 30 °C

is lowered can be ascribed either to the changes in the charge density of the surfaces or to the role played by hydrogen ions in the reactions, whilst the decrease at higher H^+ concentration points towards the role of thioglycolate anion in the dissolution mechanism.

The variation of surface charge density (σ_0) and the potential (ζ) of magnetite with pH are presented in Figure 7. These data are taken from previous work.[25] The evidence from Figure 7 shows that the fraction of protonated sites, $FeOH_2^+$, increases notably with lowering pH $\leqslant$5, even though the ζ values do not change much. Associated sites of the type $FeOH_2^+ \cdots L^-$ are even more important.[25] The adsorption of thioglycolate ions (L^-) certainly changes the electrical balance in the double layer,[12,13] but experimental data on the system cannot be given because of the changing nature of the interface during the course of the reaction. However, from the apparent affinity of thioglycolic acid shown in Figure 5 (and assuming the anion to be the adsorbate, see below), and using interface parameters for the Fe_3O_4–H_2O system in the absence of thioglycolic acid, the

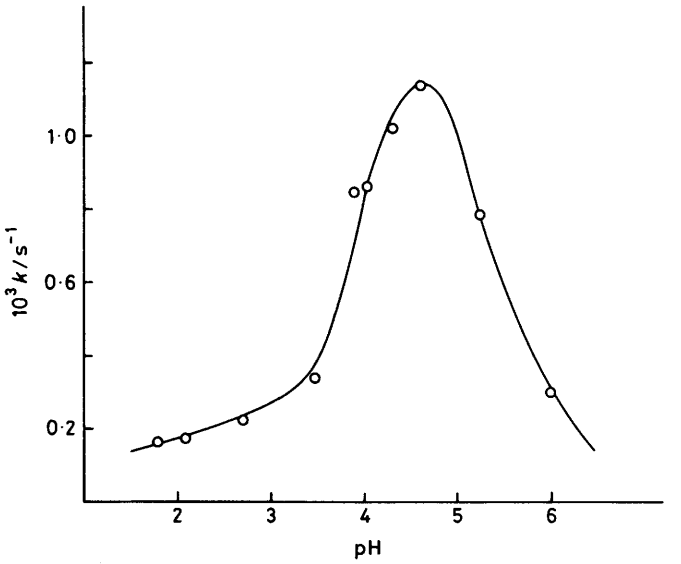

FIGURE 6 Influence of pH on the dissolution rate constant k of magnetite at 30 °C. $[HSCH_2CO_2H]$ = 0.735 mol dm^{-3}

simplified Scheme A of reaction can be written, where FeOH represents OH groups on the surface of hydrated magnetite particles and where $FeOH_2^+L^-$ represents a

$$FeOH_2^+ \rightleftharpoons FeOH + H^+ \quad K_{a_1} \quad (II)$$
$$FeOH \rightleftharpoons FeO^- + H^+ \quad K_{a_2} \quad (III)$$
$$HL \rightleftharpoons L^- + H^+ \quad K_{a_3} \quad (IV)$$
$$FeOH_2^+ + L^- \rightleftharpoons FeOH_2^+L^- \quad K_{ads.} \quad (V)$$
$$FeOH_2^+L^- \xrightarrow{slow} \text{products } [Fe^{II}, Fe^{III}, (HO_2CCH_2S)_2] \quad (VI)$$
$$\text{Rate} = k_{VI}[FeOH_2^+L^-] = k_{VI}K_{ads.}[FeOH_2^+][L^-] \quad (7)$$

SCHEME A

species containing a thioglycolate anion in the inner Helmholtz plane.[26,27] In the interaction described by equilibrium (V), there is an important electrostatic contribution, but additional specific (chemical) interactions cannot be ruled out for a complex anion such as thioglycolate.

Equilibrium (III) has been included in this Scheme for the sake of completeness, but under our conditions it has no practical significance, since no kinetic experiments were performed above pH 6, and only above pH *ca.* 6.8 (point of zero charge) the surface becomes negatively charged (see Figure 7).

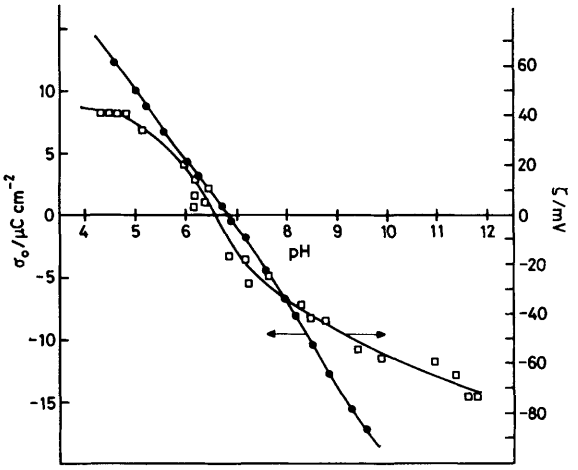

FIGURE 7 Surface charge density σ_0 (●) at ionic strength 0.1 mol dm^{-3} and potential ζ (□) of magnetite as a function of pH. T = 30 °C

Reaction (II) has been assumed to be fast. This is in agreement with previous findings, both in our laboratories and by de Bruyn and co-workers [28] and by Breeuwsma.[29] In particular, Breeuwsma has shown that surface acid–base equilibria are established rapidly, whilst bulk diffusion in the solid phase gives rise to further, much slower changes. This is the basis of the fast titration technique now currently employed, which has been applied to the present system, the findings confirming the assumption made above.

The passage from $FeOH_2^+L^-$ to ' products ' [reaction (VI)] involves a complex series of chemical changes through which oxide ion (as hydroxide or water),[30] Fe^{II}, and Fe^{III} are transferred to the bulk. Subsequent chemical changes in solution have been described by Leussing and Kolthoff,[15] but have not been included here, as they do not bear relation to the dissolution kinetics.

The relationship between thioglycolate anion concentration and analytical concentration of reagent C_L is shown in equation (8); a similar expression (9) can be

$$[L^-] = K_{a_3}C_L/([H^+] + K_{a_3}) \quad (8)$$
$$[FeOH_2^+] = [H^+]C_S/([H^+] + K_{a_1}) \quad (9)$$

written for $[FeOH_2^+]$ as a function of concentration of total available sites, C_S,[26] where C_S is given in ' mol-number ' of sites per cm^2. Actually, equation (9) is valid only if $[H^+]$ is the activity of H^+ in the interface, which is related to bulk pH through equation (10), where ψ_0 is the potential at the interface.

$$[H^+]_{interface} = [H^+]_{bulk} \cdot \exp(-e\psi_0/kT) \quad (10)$$

In practice, this means that $[FeOH_2^+]$ changes with bulk pH less markedly than as predicted by equation (9), but considering that the present experiments have been carried out at rather high ionic strengths, this correction can be safely ignored.

From equations (7), (8), and (9), the equation (11) for the reaction rate is obtained.

$$\text{Rate} = k_{VI}K_{ads.}\{K_{a_3}/([H^+] + K_{a_3})\}\{[H^+]/([H^+] + K_{a_1})\}C_LC_S \quad (11)$$

It is instructive to work out the rate–pH dependence at fixed C_L and C_S, for different relative values of K_a and K_{a_3}. In every case, the rate–pH profile shows a maximum, as shown in Figure 6. The relationship of $k_{exp.}$ (experimental rate constant) to elementary k_{VI} and K values is however different, according to the relative values of K_{a_1} and K_{a_3}. This is shown in the Table.

Analysis of equation (11): values of maximum $k_{exp.}$ for different relative values of K_{a_1} and K_{a_3}

Condition	$k_{exp.}$ (maximum)	$[H^+]$ (at the maximum)
$K_{a_1} \ll K_{a_3}$	$k_{VI}K_{ads.}$	$K_{a_1} \ll [H^+]_{max.} \ll K_{a_3}$
$K_{a_1} = K_{a_3} = K$	$k_{VI}K_{ads.}/4$	K
$K_{a_1} \gg K_{a_3}$	$k_{VI}K_{a_3}K_{ads.}/K_{a_1}$	$K_{a_3} \ll [H^+]_{max.} \ll K_{a_1}$

Typical curves for each case are shown in Figure 8, where the relative values of K_{a_1} and K_{a_3} have been taken in such a way that the maxima are located at pH 4.5. If these curves are normalized with respect to the curve $k_{exp.}$ *versus* pH, that is their maxima are made coincident with the maximum experimental k value (1.14×10^{-3} s^{-1} at pH 4.5), the curves shown in Figure 9 are obtained. An interesting feature of these curves is that for any ratio $K_{a_1} : K_{a_3}$, the same curve is obtained, whether the ratio or its inverse is used in the calculations. An analysis of these curves, together with the values of $k_{exp.}$ also included in Figure 9, leads to the conclusion that the relative values of K_{a_1} and K_{a_3} are limited to $K_{a_1} = 10^2K_{a_3}$ or the inverse ($K_{a_1} = 10^{-2}K_{a_3}$). By taking into consideration the position of the maximum, the absolute values of both K_{a_1} and K_{a_3} must therefore be between the limits 3.16×10^{-4} and 3.16×10^{-6} mol dm^{-3}. When using

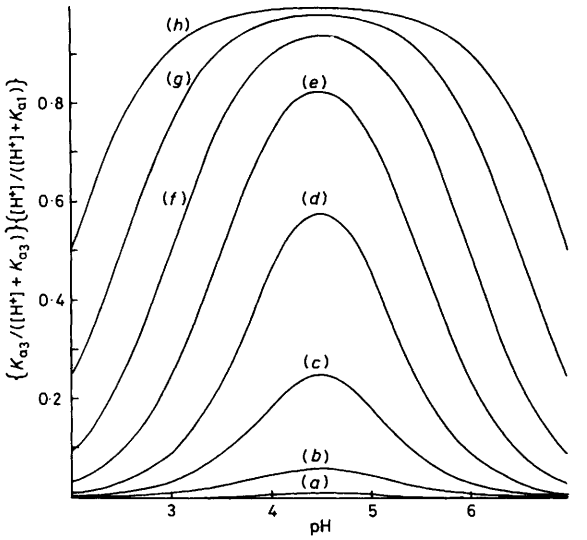

FIGURE 8 Dependence of the dissolution rate constant k of magnetite on pH, according to the term $\{K_{a_2}/([H^+] + K_{a_2})\}$-$\{[H^+]/([H^+] + K_{a1})\}$ of equation (11), for different values of the ratio $K_{a_1} : K_{a_2}$: curve (*a*) 10^2, (*b*) 10, (*c*) 1, (*d*) 10^{-1}, (*e*) 10^{-2}, (*f*) 10^{-3}, (*g*) 10^{-4}, and (*h*) 10^{-5}

the well known value of 3.16×10^{-4} mol dm^{-3} for K_{a_2},[31] the preceding analysis, based on kinetic data, gives a value of 3.16×10^{-6} mol dm^{-3} for K_{a_1}. This value cannot be obtained directly from experimental data, but can be evaluated in principle by analysis of potentiometric titration data using modern models of the oxide–water interface;[26,27] this is being currently carried out in our laboratories, a value of $K_{a_1} = 4 \times 10^{-5}$ mol dm^{-3} being obtained. This value is an order of magnitude larger than the value obtained through the kinetic analysis, but the approximations inherent in both the kinetic and thermodynamic models should explain this difference. If a simpler model for the interaction between ions and the oxide–water interface is used (see ref. 32), a value of 6.3×10^{-6} mol dm^{-3} for K_{a_1} is obtained at ionic strength

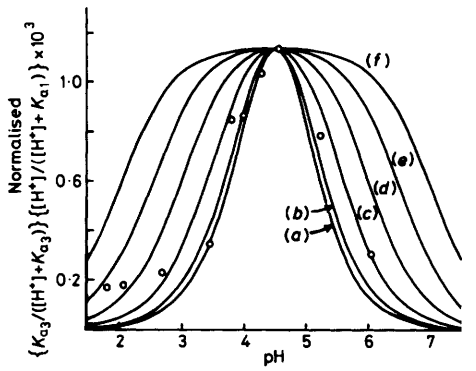

FIGURE 9 Dependence of the dissolution rate constant k of magnetite on pH, according to the term $\{K_{a_2}/([H^+] + K_{a_2})\}$-$\{[H^+]/([H^+] + K_{a_1})\}$ of equation (11), for different values of the ratio $K_{a_1} : K_{a_2}$ (curves have been normalized by equating the values at the maxima to the maximum experimental k value): (*a*) 1, (*b*) 10 and 10^{-1}, (*c*) 10^2 and 10^{-2}, (*d*) 10^3 and 10^{-3}, (*e*) 10^4 and 10^{-4}, and (*f*) 10^5 and 10^{-5}; (○) experimental values

0.1 mol dm^{-3} (much closer to 3.16×10^{-6} mol dm^{-3}). Furthermore, in this model, at higher ionic strength a lower K_{a_1} is expected.

Other possible reaction schemes should be considered in view of the ideas advanced by Vermilyea[30] for the dissolution of ionic oxides, which involve a dependence of the composite process (VI) with pH. Such a scheme, shown below, does not yield the adequate rate constant dependence on pH; it should be concluded that in the present system $[H^+]$ does not influence the value of k_{VI}.

In Scheme B the adsorption sites are considered to be more than 80% in the non-dissociated state, FeOH, and their number is taken as approximately equal to the total number of sites, C_S. Equation (12) gives a rate–

$$\begin{aligned} &HL \rightleftharpoons L^- + H^+ \quad K_{a_2} \quad (IV)\\ &FeOH + L^- \rightleftharpoons FeOHL^- \quad K_{ads.} \quad (VII)\\ &FeOHL^- + H^+ \xrightarrow{slow} \text{products} \quad (VIII)\\ &\text{Rate} = k_{VIII}[FeOHL^-][H^+]\\ &\quad = k_{VIII}K_{ads.}\{K_{a_2}/([H^+] + K_{a_2})\}[H^+]C_S C_L \quad (12) \end{aligned}$$

SCHEME B

pH curve levelling off at low pH values, with no maximum.

The results reported here have a more general significance, as the main features seem to be present in many cases of dissolution of iron oxides by organic acids. Particularly important are the cases of H_4edta, to be discussed in a future paper, and oxalic acid, which seems to be amongst the best reagents for dissolution of iron oxides. Therefore, it should be expected in general that under non-stagnant conditions (where mass transfer is definitely not rate-controlling), the rate of dissolution will be governed by the amount of oxide surface area available, by the free energy of adsorption of the reagent anion, and also by the best compromise between the pH dependences of attacking anion concentration and adequate protonation of the oxide surface. In future publications we shall discuss other cases of practical importance.

The influence of pH on the surface can also be seen

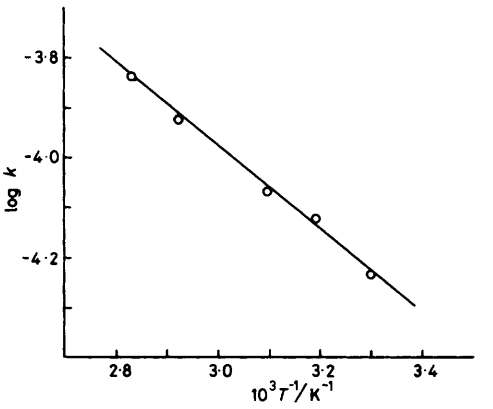

FIGURE 10 Temperature dependence of the dissolution rate constant k of magnetite at pH 4.0; $[HSCH_2CO_2H] = 0.524$ mol dm^{-3}

isolated from its effect on the deprotonation of the ligand in the reduction of iron(III) oxide by V^{II} complexes, studied by Segal and Sellers.[8]

The temperature dependence of the rate constant of dissolution of magnetite by thioglycolic acid is shown in Figure 10. The data shown there refer to pH 4.0 (25 °C). From them, an apparent activation enthalpy of 15.5 kJ mol^{-1} is calculated.

It should be clear that in the present study we have combined in the slow step several possible (and perhaps necessary) phenomena taking place at the disintegrating interface.[21] The only conclusion on this aspect from our data is that surface regeneration must be fast, compared with the time-scale of the dissolution measurements.

The authors are grateful to Dr. H. Isaurralde for collaborating during the early stages of this research and to N. de Titto for his contribution to the experimental work.

[1/1856 *Received*, 30*th November*, 1981]

REFERENCES

[1] T. W. Swaddle and P. Oltmann, *Can. J. Chem.*, 1980, **58**, 1763.
[2] T. E. Rummery, J. J. Hawton, and D. Owen, *Corrosion*, 1977, **33**, 369 and refs. therein.
[3] A. M. Olmedo, M. Villegas, M. A. Blesa, R. Fernández Prini, and A. J. G. Maroto, presented in part at the Interamerican Conference on Materials Technology, Mexico, 1981.
[4] J. A. Ayres, 'Decontamination of Nuclear Reactors and Equipment,' Ronald Press, New York, 1970.
[5] W. J. Blume, *Mater. Perform.*, 1977, **16**, 15.
[6] A. B. Johnson, jun., B. Griggs, and J. F. Remark, *Corrosion* 78, paper 38, Houston, National Association of Corrosion Engineers, 1978.
[7] A. B. Johnson, jun., B. Griggs, F. M. Kustas, and R. A. Shaw, in 'Water Chemistry of Nuclear Reactor Systems,' ed. British Nuclear Energy Society, 1980, vol. 2, p. 273; H. J. Schroeder, *ibid.*, p. 261.
[8] M. G. Segal and R. M. Sellers, *J. Chem. Soc., Chem. Commun.*, 1980, 991.
[9] F. H. Sweeton, C. F. Baes, and G. H. Jenks, *Am. Nucl. Soc. Trans.*, 1969, **12**, 82; P. R. Tremaine, R. von Massow, and G. R. Shierman, *Thermochim. Acta*, 1977, **19**, 287.
[10] E. Baumgartner and D. H. Lister, presented in part at the Int. Conf. on Decontamination of Nuclear Facilities, Niagara Falls, Canada, 1982.
[11] J. Rubio and E. Matijević, *J. Colloid Interface Sci.*, 1979, **68**, 408.
[12] A. E. Regazzoni, M. A. Blesa, and A. J. G. Maroto, unpublished work.
[13] M. A. Blesa, E. B. Borghi, H. A. Marinovich, A. J. G. Maroto, P. J. Morando, and A. E. Regazzoni, presented in part at the 10th Scientific Meeting of the Argentine Nuclear Technology Association, Bahía Blanca, 1981.
[14] E. Lyons, *J. Am. Chem. Soc.*, 1927, **49**, 1916.
[15] D. L. Leussing and I. M. Kolthoff, *J. Am. Chem. Soc.*, 1953, **75**, 390.
[16] D. L. Leussing and L. Newman, *J. Am. Chem. Soc.*, 1956, **78**, 552.
[17] A. E. Regazzoni, G. A. Urrutia, M. A. Blesa, and A. J. G. Maroto, *J. Inorg. Nucl. Chem.*, 1981, **43**, 1489.
[18] M. A. Blesa, A. J. G. Maroto, S. I. Passagio, F. Labenski, and C. Saragovi-Badler, *Radiat. Phys. Chem.*, 1978, **11**, 321.
[19] A. M. Pritchard and B. T. Mould, *Corrosion Sci.*, 1971, **11**, 1; A. M. Pritchard, J. R. Haddon, and G. N. Walton, *ibid.*, p. 11.
[20] A. J. G. Maroto, M. A. Blesa, A. E. Regazzoni, and G. A. Urrutia, in 'Water Chemistry of Nuclear Reactor Systems,' ed. British Nuclear Energy Society, 1980, vol. 2, p. 171.
[21] W. E. Dibble, jun., and W. A. Tiller, *Geochim. Cosmochim. Acta*, 1981, **45**, 79.
[22] M. E. Wadsworth in 'Physical Chemistry. An Advanced Treatise,' ed. H. Eyring, Academic Press, New York, 1975, vol. 7, p. 413.
[23] D. Bradbury, in 'Water Chemistry of Nuclear Reactor Systems,' ed. British Nuclear Energy Society, 1978, vol. 1, p. 373.
[24] G. W. Castellan, 'Physical Chemistry,' Addison-Wesley, Reading, Massachusetts, 1971, ch. 33.
[25] A. J. G. Maroto, M. A. Blesa, S. I. Passagio, and A. E Regazzoni, in 'Water Chemistry of Nuclear Reactor Systems,' ed. British Nuclear Energy Society, 1981, vol. 2, p. 177; M. A. Blesa, R. E. Larotonda, A. J. G. Maroto, and A. E. Regazzoni, *Colloids Surfaces*, submitted for publication; see also P. H. Tewari and A. W. McLean, *J. Colloid Interface Sci.*, 1972, **40**, 267.
[26] J. A. Davis, R. O. James, and J. O. Leckie, *J. Colloid Interface Sci.*, 1978, **67**, 90.
[27] J. A. Davis, R. O. James, and J. O. Leckie, *J. Colloid Interface Sci.*, 1978, **63**, 480.
[28] Y. G. Berubé, G. Y. Onoda, and P. L. de Bruyn, *Surface Sci.*, 1967, **8**, 448; G. Y. Onoda and P. L. de Bruyn, *ibid.*, 1966, **4**, 48.
[29] A. Breeuwsma, Ph.D. Thesis, Agricultural University, Wageningen, The Netherlands, 1973.
[30] D. A. Vermilyea, *J. Electrochem. Soc.*, 1966, **113**, 1067.
[31] 'Critical Stability Constants,' ed. A. M. Martell and R. M. Smith, Plenum Press, New York, 1977, vol. 3.
[32] L. Sigg and W. Stumm, *Colloids Surfaces*, 1981, **2**, 101; W. Stumm, C. P. Huang, and S. R. Jenkins, *Croat. Chem. Acta*, 1970, **42**, 223.